
Article:
Chen, H., Wang, W. and Liu, W. orcid.org/0000-0003-2968-2888 (2020) Augmented quaternion ESPRIT-type DOA estimation with a crossed-dipole array. IEEE Communications Letters, 24 (3). pp. 548-552. ISSN 1089-7798

https://doi.org/10.1109/lcomm.2019.2962463

Augmented Quaternion ESPRIT-Type DOA Estimation with a Crossed-Dipole Array

Hua Chen, *Member, IEEE,* Weifeng Wang, and Wei Liu, *Senior Member, IEEE*

***Abstract*—In this paper, a quaternion-based ESPRIT-type algorithm called augmented quaternion ESPRIT (AQ-ESPRIT) is proposed for direction of arrival (DOA) estimation with a co-located crossed-dipole array. Firstly, two quaternion models are constructed by judiciously arranging the observed signals, and then concatenated to form a new AQ model. Secondly, the AQ signal subspace is estimated by applying the quaternionic eigenvalue decomposition to the resultant AQ covariance matrix. Finally, the derived AQ signal subspaces of different subarrays are employed to form the rotational invariance equation, which is then used to obtain the ultimate DOA estimates. Numerical results show that the proposed AQ-ESPRIT has a better performance in low signal-to-noise ratio scenarios.**

***Index Terms*—Direction of arrival, augmented quaternion, co-located crossed-dipole, ESPRIT.**

I. Introduction

LOCALIZATION of multiple noise-corrupted electromagnetic (EM) signals is a fundamental problem in scalar-array and vector-array signal processing, which has found many applications in radar, sonar, and wireless communications, etc.[1–3]. Many successful subspace-based algorithms such as MUSIC and ESPRIT have been directly extended to vector-array signal processing through a 'long vector' approach [4–6], achieving superior performance over their scalar-array counterparts by simultaneously exploiting the spatial-temporal-polarimetric information.

One drawback of the 'long vector' approach is that it ignores the structural information provided by vector arrays, there have been some efforts made to model the signals based on the quaternion theory [7–9]. Following the subspace-based direction of arrival (DOA) estimation method, a quaternion MUSIC (Q-MUSIC) algorithm was proposed in [7] with a quaternion formulation of a two-component vector-array, which requires half of the memory size for the data covariance matrix compared to the long vector model. By employing a three-component vector array with the recorded signals expressed as biquaternion values, a biquaternion MUSIC (BQ-MUSIC) algorithm was derived based on the projected noise subspace by performing the eigenvalue decomposition (EVD) of a Hermitian biquaternion matrix [8]. Furthermore, Gong et al. proposed a quad-quaternion model in [9] to characterize the observed signal of a six-component vector array, which leads to a quad-quaternion MUSIC (QQ-MUSIC) algorithm with strong quad-quaternion orthogonality restrictions. These hypercomplex-valued MUSIC methods have demonstrated their superiority over the long vector solution in terms of subspace estimation performance and robustness to model errors. However, these hypercomplex-valued MUSIC methods suffer from its heavy computational burden due to the multidimensional peak-search process. Given its high computational efficiency, the traditional ESPRIT algorithms have been extended into both the long vector form [10] and the quaternion form [11, 12]. The quaternion ESPRIT (Q-ESPRIT) algorithm was firstly proposed in [11] for a crossed-dipole uniform linear array (ULA), which takes advantage of the underlying rotational invariance property between signal subspaces of different subarrays. Then, the one-dimensional (1-D) Q-ESPRIT was further extended to two-dimensional (2-D) ones based on the co-located crossed-dipole (CCD) array [12].

In this paper, an augmented quaternion ESPRIT (AQ-ESPRIT) algorithm is proposed based on a CCD ULA by concatenating two quaternion models into an AQ model. Then, the AQ covariance matrix is calculated and the quaternionic eigenvalue decomposition (QEVD) is applied to obtain the AQ signal subspace. The parameters of interest can then be estimated based on the rotational invariance equation. The performance of the proposed algorithm is compared with its existing ESPRIT-type counterparts through computer simulations, showing an improved performance, especially in low signal-to-noise ratio (SNR) scenarios.

Throughout the paper, the notations $(\cdot)^*$, $(\cdot)^T$, $(\cdot)^{-1}$, and $(\cdot)^H$ represent conjugation, transpose, inverse, and conjugate transpose, respectively. $diag\{\cdot\}$ and $blkdiag[\cdot,\cdot]$ denote the diagonal and block diagonal matrices, respectively; $[\cdot;\cdot]$ denotes the extended matrix column-stacked with two matrices; $E(\cdot)$ is the expectation operator; $arg(\cdot)$ is the phase operation; $\mathbf{I}_p$ denotes the p-dimensional identity matrix; $\otimes$ and $\odot$ are the Kronecker product and Hadamard product operations, respectively. $\mathbf{0}_p$ and $\mathbf{1}_p$ denote all-zero and all-one $p \times 1$ row

Manuscript received August 07, 2019; revised *** **, 2019; accepted *** **, 2019. Date of publication *** **, 2019; date of current version *** **, 2019. The associate editor coordinating the review of this manuscript and approving it for publication was Dr. ** **. (*Corresponding author: Hua Chen and Wei Liu.*)

This work is sponsored by the Key Laboratory of Intelligent Perception and Advanced Control of State Ethnic Affairs Commission under Grant MD-IPAC-2019102, and by Zhejiang Provincial Natural Science Foundation of China under Grants LQ19F010002 and LR20F010001, and by Natural Science Foundation of Ningbo Municipality under Grant 2018A610094, and by the National Natural Science Foundation of China under Grants 61871282 and 61871245, and by K. C. Wong Magna Fund in Ningbo University.

Hua Chen is with the Faculty of Information Science and Engineering, Ningbo University, Ningbo, 315211, China, and also with the Key Laboratory of Intelligent Perception and Advanced Control of State Ethnic Affairs Commission, Dalian 116600, China.(e-mail: dkchenhua0714@hotmail.com)

Weifeng Wang is the 54th Research Institute of China Electronics Technology Group Corporation (CETC54).

Wei Liu is with the Department of Electronic and Electrical Engineering, University of Sheffield, Sheffield, UK S1 3JD.(e-mail: w.liu@sheffield.ac.uk)

vectors, respectively. $\mathbb{R}$, $\mathbb{C}$, and $\mathbb{H}$ represent real, complex and quaternion field, respectively.

II. Basics of Quaternions

A quaternion q consists of one real part and three imaginary components, which can be expressed in its Cayley-Dickson form as [7, 13]:

$$\begin{aligned} q &= r_0 + r_1 i + r_2 j + r_3 k \\ &= c_1 + c_2 j, \end{aligned} \tag{1}$$

where $r_0, r_1, r_2, r_3 \in \mathbb{R}$ are real numbers, $c_1 = r_0 + r_1 i, c_2 = r_2 + r_3 i \in \mathbb{C}$ are complex numbers, and i, j, k are three imaginary units satisfying:

$$\begin{aligned} &ij = -ji = k, \qquad jk = -kj = i, \\ &ki = -ik = j, \qquad i^2 = j^2 = k^2 = -1. \end{aligned} \tag{2}$$

Although several properties of complex numbers can be extended to quaternions directly, there are still some unique properties which will be used in this paper [14–16]:

• The conjugate of a quaternion q is denoted by $q^* = r_0 - r_1 i - r_2 j - r_3 k$.

• The module of a quaternion q is $|q| = \sqrt{qq^*} = \sqrt{r_0^2 + r_1^2 + r_2^2 + r_3^2}$.

• Given two quaternions q_1 and q_2, we normally have $q_1 q_2 \neq q_2 q_1$.

• Conjugation over $\mathbb{H}$ is an anti-involution, which means $(q_1 q_2)^* = q_2^* q_1^*$.

As with complex matrices, we define the matrix consisting of quaternions as quaternion matrix. Similarly, we introduce some necessary definitions and properties of a quaternion matrix used in our proposed algorithm.

• The Cayley-Dickson notation for a quaternion matrix $\mathbf{B} \in \mathbb{H}^{M\times N}$ can be written as $\mathbf{B} = \mathbf{B}_1 + \mathbf{B}_2 j, (\mathbf{B}_1, \mathbf{B}_2 \in \mathbb{C}^{M\times N})$. Then one can define the complex adjoint matrix, denoted by $\mathbf{B}^\sigma$, corresponding to the quaternion matrix, as follows

$$\mathbf{B}^\sigma = \begin{bmatrix} \mathbf{B}_1 & \mathbf{B}_2 \\ -\mathbf{B}_2^* & \mathbf{B}_1^* \end{bmatrix} \tag{3}$$

• A quaternion square matrix $\mathbf{B} \in \mathbb{H}^{M\times M}$ satisfying $\mathbf{B} = \mathbf{B}^H$ is called a Hermitian matrix. The eigenvalues of a Hermitian matrix are real numbers, and they are the eigenvalues of the complex adjoint matrix $\mathbf{B}^\sigma$ as well.

• Given a square quaternion matrix $\mathbf{B} \in \mathbb{H}^{M\times M}$, the eigenvalue decomposition of its adjoint matrix $\mathbf{B}^\sigma$ can be expressed as:

$$\mathbf{B}^\sigma = \begin{bmatrix} \mathbf{U}_1 & \mathbf{U}_2 \\ -\mathbf{U}_2^* & \mathbf{U}_1^* \end{bmatrix} \begin{bmatrix} \mathbf{D} & \mathbf{0} \\ \mathbf{0} & \mathbf{D}^* \end{bmatrix} \begin{bmatrix} \mathbf{U}_1 & \mathbf{U}_2 \\ -\mathbf{U}_2^* & \mathbf{U}_1^* \end{bmatrix}^H = \mathbf{U}_c \mathbf{D}_c \mathbf{U}_c^H, \tag{4}$$

where $\mathbf{D} \in \mathbb{H}^{M\times M}$ contains the complex eigenvalues of $\mathbf{B}^\sigma$. It is clear that the eigenvalues of $\mathbf{B}^\sigma$ appear in conjugated pairs, $\mathbf{D}_c$ and $\mathbf{U}_c$ are the adjoint matrices of $\mathbf{D}$ and $\mathbf{U} = \mathbf{U}_1 + \mathbf{U}_2 j$, respectively. In particular, when $\mathbf{B}$ is a Hermitian matrix, $\mathbf{D}$ is a real diagonal matrix. Therefore, the eigenvalue decomposition of the quaternion matrix $\mathbf{B}$ is given by

$$\mathbf{B} = (\mathbf{U}_1 + \mathbf{U}_2 j)\mathbf{D}(\mathbf{U}_1 + \mathbf{U}_2 j)^H. \tag{5}$$

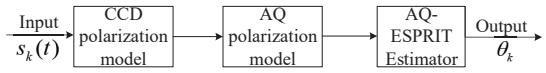

Fig. 1. The system diagram of the proposed method.

III. Augmented Quaternion ESPRIT Algorithm

In this section, we first introduce the CCD polarization model for fully polarized signals received by a two-component vector array, and then the AQ polarization model is built, followed by the proposed AQ ESPRIT. The system diagram of the proposed method is illustrated in Fig. 1.

A. CCD polarization model

As shown in Fig. 2, consider a CCD ULA of M elements with K far-field uncorrelated fully polarized signals $s_k(t), k = 1, \cdots, K$, impinging from DOA angles θ_k. The CCD array is deployed in the y-axis with its mth element located at $md, m = 0, \cdots M-1$, where d is the distance between two adjacent elements. Each polarization component of the cross-dipoles can measure the electric field along x and y axes in the y-z plane, respectively, as [10]

$$\boldsymbol{\xi}_k = \begin{bmatrix} \xi_{k1} \\ \xi_{k2} \end{bmatrix} = \begin{bmatrix} 1 & 0 \\ 0 & \cos\theta_k \end{bmatrix} \begin{bmatrix} \cos\alpha_k \\ \sin\alpha_k e^{i\beta_k} \end{bmatrix}, \tag{6}$$

where $0 \le \alpha_k \le \pi/2$ and $0 \le \beta_k \le 2\pi$ are the polarization angle and phase difference, respectively. The two-component data vector measured by the mth cross-dipole at time t can be expressed as

$$\mathbf{x}_m(t) = \begin{bmatrix} x_{1m}(t) \\ x_{2m}(t) \end{bmatrix} = \sum_{k=1}^{K} a_m(\theta_k)\boldsymbol{\xi}_k s_k(t) + \begin{bmatrix} n_{1m}(t) \\ n_{2m}(t) \end{bmatrix}, \tag{7}$$

where $a_m(\theta_k) = e^{-i(2\pi md/\lambda)\sin\theta_k}$, λ is the wavelength, and $n_{1m}(t)$ and $n_{2m}(t)$ are the additive white Gaussian noise of the mth cross-dipole antennas, respectively.

B. AQ polarization model

In order to exploit the orthogonal structure of the crossed-dipole array, we define a quaternion as

$$\bar{q}_k(\alpha_k, \beta_k) = \cos\alpha_k + j\cos\theta_k \sin\alpha_k e^{i\beta_k}. \tag{8}$$

The associated two-component quaternion observed signal $\bar{x}_m(t)$ is then given by

$$\begin{aligned} \bar{x}_m(t) &= x_{1m}(t) + j x_{2m}(t) \\ &= \sum_{k=1}^{K} a_m(\theta_k)\bar{q}_k(\alpha_k, \beta_k)s_k(t) + \bar{n}_m(t), \end{aligned} \tag{9}$$

where $\bar{n}_m(t) = n_{1m}(t) + j n_{2m}(t)$. By stacking $\bar{x}_m(t), m = 0, \cdots M-1$ into a column, we have

$$\bar{\mathbf{x}}(t) = \mathbf{A}\bar{\mathbf{Q}}\mathbf{s}(t) + \bar{\mathbf{n}}(t), \tag{10}$$

where $\mathbf{A} = [\mathbf{a}_1, \cdots, \mathbf{a}_K]$ is the array manifold with each column denoted by $\mathbf{a}_k = [1, \cdots, a_M(\theta_k)]^T$, $\bar{\mathbf{Q}} = diag\{\bar{q}_1, \cdots, \bar{q}_K\}$, $\bar{\mathbf{n}}(t) = [\bar{n}_0(t), \cdots, \bar{n}_{M-1}(t)]^T$ and $\mathbf{s}(t) = [s_1(t), \cdots, s_K(t)]^T$. Similarly, by swapping the order of the

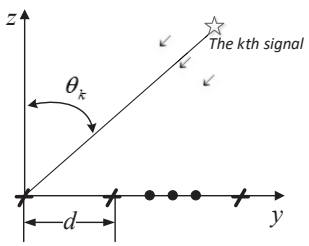

Fig. 2. The geometry of the CCD array model.

two components, we define another quaternion as

$$\underline{q}_{\underline{k}}(\alpha_k, \beta_k) = \cos\theta_k \sin\alpha_k e^{i\beta_k} + j\cos\alpha_k. \tag{11}$$

The associated observed signal $\underline{x}_m(t)$ has the form of

$$\underline{x}_m(t) = \sum_{k=1}^{K} a_m(\theta_k)\underline{q}_{\underline{k}}(\alpha_k, \beta_k)s_k(t) + \underline{n}_m(t), \tag{12}$$

where $\underline{n}_m(t)$=$n_{2m}(t)$+$jn_{1m}(t)$ and in matrix form, we have

$$\underline{\mathbf{x}}(t) = \mathbf{A}\underline{\mathbf{Q}}\mathbf{s}(t) + \underline{\mathbf{n}}(t), \tag{13}$$

where $\underline{\mathbf{Q}} = diag\{\underline{q}_1, \cdots, \underline{q}_K\}$ and $\underline{\mathbf{n}}(t) = [\underline{n}_0(t), \cdots, \underline{n}_{M-1}(t)]^T$.

C. AQ-ESPRIT estimator

To proceed, an AQ output $\mathbf{z}(t)$ of the array can be concatenated by $\bar{\mathbf{x}}(t)$ and $\underline{\mathbf{x}}(t)$

$$\begin{aligned}\mathbf{z}(t) = \begin{bmatrix} \bar{\mathbf{x}}(t) \\ \underline{\mathbf{x}}(t) \end{bmatrix} &= \begin{bmatrix} \mathbf{A}\bar{\mathbf{Q}} \\ \mathbf{A}\underline{\mathbf{Q}} \end{bmatrix}\mathbf{s}(t) + \begin{bmatrix} \bar{\mathbf{n}}(t) \\ \underline{\mathbf{n}}(t) \end{bmatrix} \\ &= \tilde{\mathbf{A}}\mathbf{s}(t) + \tilde{\mathbf{n}}(t).\end{aligned} \tag{14}$$

The quaternionic covariance matrix $\mathbf{R}$ of $\mathbf{z}(t)$ is calculated by

$$\mathbf{R} = E\left[\mathbf{z}(t)\mathbf{z}^H(t)\right] = \tilde{\mathbf{A}}\mathbf{R}_s\tilde{\mathbf{A}}^H + 2\sigma_n^2\mathbf{I}_{2M}, \tag{15}$$

σ_n^2 is the variance of noise, by performing QEVD on $\mathbf{R}$, one can obtain

$$\mathbf{R} = \mathbf{U}_s\mathbf{\Lambda}_s\mathbf{U}_s^H + \mathbf{U}_n\mathbf{\Lambda}_n\mathbf{U}_n^H, \tag{16}$$

where the $2M \times K$ quaternion matrix $\mathbf{U_s}$ and the $(2M-K)\times K$ quaternion matrix $\mathbf{U_n}$ are the signal and noise subspaces associated with corresponding eigenvalue matrices $\mathbf{\Lambda}_s$ and $\mathbf{\Lambda}_n$, respectively.

According to the subspace principle, the AQ direction matrix $\tilde{\mathbf{A}}$ and signal subspace $\mathbf{U_s}$ span the same subspace, and there exists a nonsingular matrix $\mathbf{T}$ that satisfies the following formulation

$$\mathbf{U_s} = \tilde{\mathbf{A}}\mathbf{T}. \tag{17}$$

Partitioning the AQ matrix $\mathbf{U_s}$ as

$$\mathbf{U}_s = \begin{bmatrix} \mathbf{U}_{s1} \\ \mathbf{U}_{s2} \end{bmatrix}, \tag{18}$$

we have

$$\mathbf{U}_{s1} = \mathbf{A}\overline{\mathbf{Q}}\mathbf{T}, \mathbf{U}_{s2} = \mathbf{A}\underline{\mathbf{Q}}\mathbf{T}. \tag{19}$$

Then, define two selection matrices

$$\mathbf{J}_a = blkdiag[\mathbf{J}_1, \mathbf{J}_1], \mathbf{J}_b = blkdiag[\mathbf{J}_2, \mathbf{J}_2], \tag{20}$$

with

$$\mathbf{J}_1 = [\mathbf{I}_{M-1}, \mathbf{0}_{M-1}], \mathbf{J}_2 = [\mathbf{0}_{M-1}, \mathbf{I}_{M-1}], \tag{21}$$

we have the rotational invariance equation by selecting the AQ direction matrix in diagonal form satisfying

$$\mathbf{J}_a\mathbf{A}_g\mathbf{\Phi}_g = \mathbf{J}_b\mathbf{A}_g \tag{22}$$

with $\mathbf{A}_g = [\mathbf{A}\overline{\mathbf{Q}}; \mathbf{A}\underline{\mathbf{Q}}]$, and $\mathbf{\Phi}_g$= $\mathbf{\Phi}$, where $\mathbf{\Phi} = diag\{e^{-i(2\pi/\lambda)\sin\theta_1}, \cdots, e^{-i(2\pi/\lambda)\sin\theta_K}\}$ is the rotational invariance matrix with the interested DOAs in its diagonal. It can be derived from (19) and (22) that

$$\mathbf{J}_a\mathbf{U}_{sg}\mathbf{T}_g^{-1}\mathbf{\Phi}_g\mathbf{T}_g = \mathbf{J}_b\mathbf{U}_{sg}, \tag{23}$$

where $\mathbf{U}_{sg} = [\mathbf{U}_{s1}; \mathbf{U}_{s2}]$, $\mathbf{T}_g = \mathbf{T}$.

By denoting

$$\mathbf{\Omega} = \mathbf{T}_g^{-1}\mathbf{\Phi}_g\mathbf{T}_g, \tag{24}$$

we obtain

$$\mathbf{\Omega} = (\mathbf{J}_a\mathbf{U}_{sg})^+(\mathbf{J}_b\mathbf{U}_{sg}), \tag{25}$$

where $(\cdot)^+$ donates the quaternion matrix pseudo-inverse with

$$(\mathbf{J}_a\mathbf{U}_{sg})^+ = [(\mathbf{J}_a\mathbf{U}_{sg})^H(\mathbf{J}_a\mathbf{U}_{sg})]^{-1}(\mathbf{J}_a\mathbf{U}_{sg})^H. \tag{26}$$

From equation Eq. (24), it is clear that the quaternion square matrix $\mathbf{\Omega}$ is similar with $\mathbf{\Phi}_g$, and thus the eigenvalues of $\mathbf{\Omega}$ are the diagonal elements of $\mathbf{\Phi}_g$. Because $\mathbf{\Omega}$ is a $2K \times 2K$ quaternion matrix, according to Theorem 6.1 in [15], the eigenvalues of the complex adjoint matrix $\mathbf{\Omega}^\sigma$ are also eigenvalues of $\mathbf{\Omega}$. Therefore, the eigenvalues of $\mathbf{\Omega}$ can be estimated by the eigendecompose of $\mathbf{\Omega}^\sigma$ based on the property in Eq. (4).

It is shown in (24) that the $2K$ eigenvalues appear in pairs, among which K different eigenvalues correspond to the eigenvalues of $\mathbf{\Phi}$, and thus the DOAs of the incident signals can be expressed as

$$\theta_k = \arcsin(\frac{-arg(e_k)}{2\pi d}), k = 1, \cdots, K, \tag{27}$$

where e_k is the complex eigenvalues of $\mathbf{\Omega}^\sigma$.

The proposed AQ algorithm can provide closed-form DOA estimates and it is summarized in Table I.

TABLE I
SUMMARY OF THE PROPOSED METHOD.

Step 1 Calculate $\mathbf{R}$ from N snapshots by $\hat{\mathbf{R}} = \frac{1}{N}\sum_{t=1}^{N}\mathbf{z}(t)\mathbf{z}^H(t)$.
Step 2 Perform QEVD on $\hat{\mathbf{R}}$ to obtain $\hat{\mathbf{U}}_s$.
Step 3 Construct $\hat{\mathbf{\Omega}}$ by applying two selection matrices to $\hat{\mathbf{U}}_s$.
Step 4 Eigendecompose $\hat{\mathbf{\Omega}}^\sigma$ to obtain the eigenvalues $\hat{e}_k$.
Step 5 Estimate the DOAs as $\hat{\theta}_k = \arcsin(\frac{-arg(\hat{e}_k)}{2\pi d})$.

Remark 1: The memory requirement for the three algorithms AQ-ESRPIT, Q-ESPRIT and LV-ESPRIT is compared

here, and the focus is mainly on the estimation of the covariance matrix. As for AQ-ESPRIT, a memory of about $8N^2$ complex numbers is required for the AQ covariance matrix, while for Q-ESPRIT and LV-ESPRIT, they are $2N^2$ and $4N^2$. The computational complexity of the three ESPRIT-based algorithms is mainly due to the estimation and EVD of the covariance matrix, and the EVD of the similar matrix of the rotational invariance matrix. For the LV-ESPRIT, the dimension of the received data matrix is $2M \times N$, where N is the number of snapshots. Thus, $(2M)^2 N$ flops are required for calculation of the covariance matrix. The dimension of the covariance matrix and the similar matrix is respectively $2M \times 2M$ and $K \times K$, and thus, the computational complexity of the EVD is of $(2M)^3$ and K^3. The computational complexity of the LV-ESPRIT is given by $C_{LV-ESPRIT} = (2M)^2 N + (2M)^3 + K^3$. For the Q-ESPRIT, the dimension of the received data matrix, the covariance matrix and the similar matrix is $M \times N$, $M \times M$ and $K \times K$, respectively. However, the EVD of the similar matrix is replaced by the EVD of its complex adjoint matrix with the dimension extended to $2K \times 2K$. Therefore, the computational complexity of the Q-ESPRIT is $C_{Q-ESPRIT} = M^2 N + M^3 + (2K)^3$. For the AQ-ESPRIT, the dimension of the received data matrix, the covariance matrix and the similar matrix is $2M \times N$, $2M \times 2M$ and $2K \times 2K$, respectively, and the EVD of the similar matrix is also replaced by the EVD of its complex adjoint matrix with the dimension extended to $4K \times 4K$. Therefore, the computational complexity of the Q-ESPRIT is $C_{AQ-ESPRIT} = (2M)^2 N + (2M)^3 + (4K)^3$. Thus, the AQ-ESPRIT requires more memory and has higher complexity than the other two methods, in return for an improved estimation accuracy as shown in the simulations part.

Remark 2: Differences between the LV-ESPRIT, Q-ESPRIT and AQ-ESPRIT methods: The LV-ESPRIT method models and concatenates the received signals as a 'long vector' in complex values, which ignores the structural information of vector output signals. To preserve locally the vector-type of the signal, the quaternion framework is utilized to model the vector output signal by the Q-ESPRIT method; however, the dimension of the signal subspace is reduced, resulting in performance degradation. For the proposed AQ-ESPRIT method, the augmented quaternion polarization model is adopted, whose signal subspace has the same dimension as the LV-ESPRIT, and double that of the Q-ESPRIT, thus leading to a better performance, especially in low SNR scenarios.

Remark 3: The CRB reported later in simulations is derived using the LV-model based on (7) as follows: Define a real-valued vector of the unknown parameters as $\boldsymbol{\xi} = \left[\begin{array}{ccc} \boldsymbol{\theta}^T & \boldsymbol{\alpha}^T & \boldsymbol{\beta}^T \end{array} \right]^T$ with $\boldsymbol{\theta} = [\theta_1, \theta_2, ..., \theta_K]^T$, $\boldsymbol{\alpha} = [\alpha_1, ..., \alpha_K]^T$, and $\boldsymbol{\beta} = [\beta_1, ..., \beta_K]^T$. Then, the $3K \times 3K$ CRB matrix for the parameter $\boldsymbol{\xi}$ estimate is given by [17, 18]

$$\mathrm{CRB}(\boldsymbol{\xi}) = \frac{\sigma^2}{2L} diag\{ \{ \ \mathrm{Re}[(\mathbf{D}^H \mathbf{P}^{\perp}_{\mathbf{A}_e} \mathbf{D}) \odot (\mathbf{1}_3 \otimes \mathbf{1}_3^T \otimes \mathbf{R}_s^T)] \ \}^{-1} \}, \tag{28}$$

where $\mathbf{A}_e = [\mathbf{a}_1 \otimes \boldsymbol{\xi}_1, \mathbf{a}_2 \otimes \boldsymbol{\xi}_2, \cdots, \mathbf{a}_K \otimes \boldsymbol{\xi}_K]$, $\mathbf{P}^{\perp}_{\mathbf{A}_e} = \mathbf{I}_{2M} - \mathbf{A}_e (\mathbf{A}_e^H \mathbf{A}_e)^{-1} \mathbf{A}_e^H$, $\mathbf{D} = [\mathbf{D}_\theta, \mathbf{D}_\alpha, \mathbf{D}_\beta]$ with $\mathbf{D}_\theta = \left[\frac{\partial \mathbf{A}_e}{\partial \theta_1}, ..., \frac{\partial \mathbf{A}_e}{\partial \theta_K} \right]$, $\mathbf{D}_\alpha = \left[\frac{\partial \mathbf{A}_e}{\partial \alpha_1}, ..., \frac{\partial \mathbf{A}_e}{\partial \alpha_K} \right]$, $\mathbf{D}_\beta = \left[\frac{\partial \mathbf{A}_e}{\partial \beta_1}, ..., \frac{\partial \mathbf{A}_e}{\partial \beta_K} \right]$.

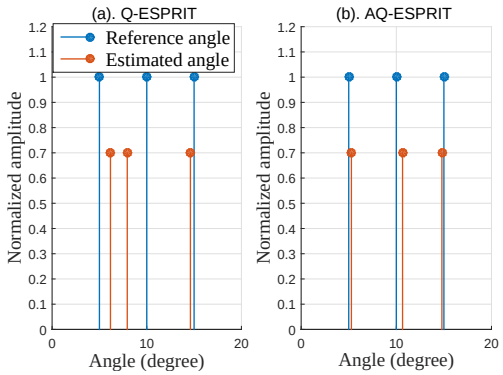

Fig. 3. An example for the spatial resolution capability.

Remark 4: When some of the incident signals are correlated, decorrelation techniques such as the classic forward-backward spatial smoothing (FBSS) will be employed as a preprocessing step before the AQ-ESPRIT method is applied. However, the FBSS operation leads to partial loss of the array aperture, which will inevitably degrade the DOA estimation performance as shown in following simulations.

IV. Simulation Results

In this section, numerical examples are provided to evaluate the performance of the proposed AQ-ESPRIT algorithm, as compared to those of LV-ESPRIT[10] and Q-ESPRIT[11]. The CRB is included as a performance benchmark. Three uncorrelated equal-power signals impinge upon a ULA of crossed dipoles with half-wavelength inter-element spacing. Three closely spaced signals are parameterized by $(\theta_1, \alpha_1, \beta_1) = (5°, 22°, 35°)$, $(\theta_2, \alpha_2, \beta_2) = (10°, 33°, 45°)$ and $(\theta_3, \alpha_3, \beta_3) = (15°, 44°, 60°)$. The noise is additive white Gaussian with zero-mean, uncorrelated with the incoming signals. The root mean squared error (RMSE) of DOA estimation, based on 2000 Monte Carlo trials, is adopted as the performance index.

In the first example, the spatial resolution capability of the Q-ESPRIT and proposed AQ-ESPRIT methods is demonstrated by a specific example based on a ULA of 4 elements. The SNR=20dB, and the number of snapshots is 800. As shown in Fig. 3, the three DOAs have been identified successfully by the AQ-ESPRIT, while large errors are introduced by the Q-ESPRIT.

In the second example, the DOA estimation performance is studied with respect to SNR. The number of elements is 8, and SNR varies from -10dB to 20dB. The number of snapshots N adopted is 100 and 10000, respectively. Fig. 4 shows the result, where it can be seen that the AQ-ESPRIT algorithm has clearly outperformed the Q-ESPRIT algorithm in low SNR regions. For example, for N=100, at SNR=6dB, the RMSE of the proposed AQ-ESPRIT algorithm is about 2 degrees better than the Q-ESPRIT algorithm.

In the third example, we evaluate the performance of the proposed method against the correlation factor ρ between $s_1(t)$ and $s_2(t)$. The other parameters are similar to those in the

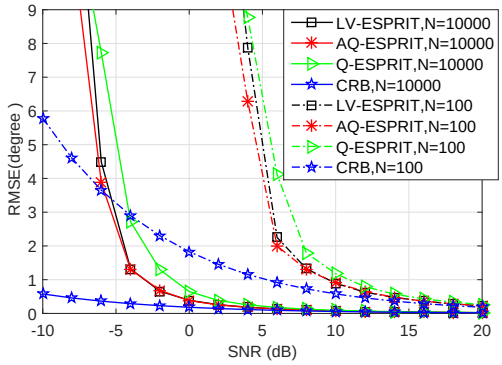

Fig. 4. RMSE versus SNR.

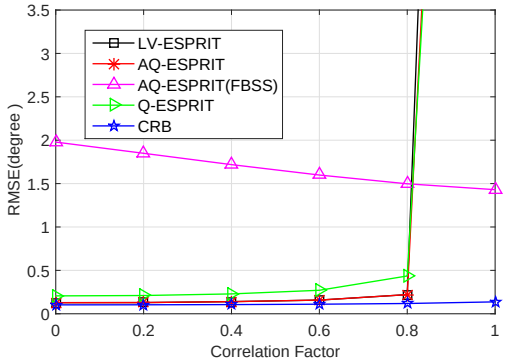

Fig. 5. RMSE versus correlation factor.

second example, except that SNR=15dB, and the number of snapshots is 1000. As shown in Fig. 5, when the correlation factor varies from 0 to 1, all the methods have suffered with a deteriorating performance, except that the AQ-ESPRIT method with FBSS which has kept a steady performance.

V. Conclusion

A new algorithm called AQ-ESPRIT has been proposed for DOA estimation of fully polarized signals with a crossed-dipole ULA. Based on the quaternion formulation, an AQ data model is constructed and by performing QEVD to the AQ covariance matrix, it is shown that the DOA estimates can be achieved via the rotational invariance equation, which is formed by the selected AQ signal subspaces related to the corresponding subarrays. In comparison with the existing ESPRIT-type counterparts, an overall improved performance has been achieved by the proposed method.

References

[1] H. L. Van Trees, *Optimum Array Processing: Part IV of Detection, Estimation, and Modulation Theory*. New York, NY, USA: Wiley, 2002.

[2] Y. Yue, Y. Xu, Z. Liu and L. Shen, "Parameter estimation of coexisted circular and strictly noncircular sources using diversely polarized antennas," *IEEE Communications Letters*, vol. 22, no. 9, pp. 1822-1825, Sept. 2018.

[3] X. Zhang, L. Xu, L. Xu, and D. Xu, "Direction of departure (DOD) and direction of arrival (DOA) estimation in MIMO radar with reduced-dimension MUSIC," *IEEE Communications Letters*, vol. 14, no. 12, pp. 1161–1163, 2010.

[4] X. Gong, J. Jiang, H. Li, Y. Xu and Z. Liu, "Spatially spread dipole/loop quint for vector-cross-product-based direction finding and polarisation estimation," *IET Signal Processing*, vol. 12, no. 5, pp. 636-642, 2018.

[5] X. Wang, L. Wan, M. Huang, C. Shen and K. Zhang, "Polarization channel estimation for circular and non-circular signals in massive MIMO systems," *IEEE Journal of Selected Topics in Signal Processing*, vol. 13, no. 5, pp. 1001-1016, Sept. 2019.

[6] H. Chen, W. Wang and W. Liu, "Joint DOA, range, and polarization estimation for rectilinear sources with a COLD array,"*IEEE Wireless Communications Letters*, vol. 8, no. 5, pp. 1398-1401, Oct. 2019.

[7] S. Miron, N. Le Bihan and J. I. Mars, "Quaternion-MUSIC for vector-sensor array processing," *IEEE Transactions on Signal Processing*, vol. 54, no. 4, pp. 1218-1229, April 2006.

[8] N. Le Bihan, S. Miron and J. I. Mars, "MUSIC algorithm for vector-sensors array using biquaternions," *IEEE Transactions on Signal Processing*, vol. 55, no. 9, pp. 4523-4533, Sept. 2007.

[9] X. Gong, Z. Liu, Y. Xu, "Quad-quaternion MUSIC for DOA estimation using electromagnetic vector sensors," *EURASIP Journal on Advances in Signal Processing*, vol. 2008, 204, 2008.

[10] J. Li and R. T. Compton, "Angle and polarization estimation using ESPRIT with a polarization sensitive array," *IEEE Transactions on Antennas and Propagation*, vol. 39, no. 9, pp. 1376-1383, Sept. 1991.

[11] X. Gong, Y. Xu and Z. Liu, "Quaternion ESPRIT for direction finding with a polarization sentive array," *2008 9th International Conference on Signal Processing*, Beijing, 2008, pp. 378-381.

[12] Y. Li, J. Q. Zhang, B. Hu, H. Zhou and X. Y. Zeng, "A novel 2-D quaternion ESPRIT for joint DOA and polarization estimation with crossed-dipole arrays,"*2013 IEEE International Conference on Industrial Technology (ICIT)*, Cape Town, 2013, pp. 1038-1043.

[13] M. D. Jiang, Y. Li, and W. Liu, "Properties of a general quaternion-valued gradient operator and its application to signal processing," *Frontiers of Information Technology Electronic Engineering*, vol. 17, issue 2, pp. 83-95, Feb. 2016.

[14] W. Wang, H. Chen, J. Jin, X. Wang, L. Wan, X. Zhang, "Quaternion-MUSIC for near-field strictly noncircular sources with large-scale polarization array," *Digital Signal Processing*, vol. 94, pp. 137-145, Nov. 2019.

[15] F. Zhang, "Quaternions and matrices of quaternions," *Linear Algebra Its Applications*, vol. 251, pp. 21-57, Jan. 1997.

[16] N. L. Bihan and J. Mars, "Singular value decomposition of quaternion matrices: a new tool for vector-sensor signal processing," *Signal Process.*, vol. 84, no. 7, pp. 1177-1199, Jul. 2004.

[17] P. Stoica, A. Nehorai, "Performance study of conditional and unconditional direction-of-arrival estimation," *IEEE Transactions on Acoustics, Speech, and Signal Processing*, vol. 38, no. 10, pp. 1783-1795, Oct. 1990.

[18] A. Nehorai and E. Paldi, "Vector-sensor array processing for electromagnetic source localization,"*IEEE Transactions on Signal Processing*, vol. 42, no. 2, pp. 376-398, Feb. 1994.